NASA CR-66842

FORM 82377-D

THE GARRETT CORPORATION
AiResearch Manufacturing Division
LOS ANGELES 45, CALIFORNIA

REPORT NO. AP-68-4617

TEST REPORT ON FATIGUE-TESTING OF NICKEL-200 PANELS HYPERSONIC RESEARCH ENGINE PROJECT - PHASE IIA NASA CONTRACT NO. NAS1-6666

NO. OF PAGES 16

DATE 10 January 1969

PREPARED BY Engineering Staff

EDITED BY F. A. Biastre

APPROVED BY Henry J. Lopez
Henry J. Lopez
HRE Program Manager

ABSTRACT

This report presents the results of fatigue tests conducted on Nickel-200 alloy to obtain low cycle thermal fatigue performance data for application to the regeneratively cooled structures on the Hypersonic Research Engine. The objective was to determine the advantages of using Ni-200 material as opposed to Hastelloy-X. The results show that the low cycle fatigue life of the engine structure would be increased from 136 cycles for Hastelloy-X up to 225 cycles for Ni-200 at the most severe design operating condition. This is due to the higher thermal conductivity and higher ductility of the Ni-200 at operating temperature as compared to Hastelloy-X. The relatively lower creep-rupture strength of the Ni-200 would not, however, permit application in structural parts under high mechanical stress.

FOREWORD

This Category I Test Report is submitted to the NASA Langley Research Center by the AiResearch Manufacturing Company, Los Angeles, California. The document was prepared in compliance with Paragraph 4.3.3.c of NASA Reliability Publication NPC250-1.

CONTENTS

ILLUSTRATIONS

TABLES

1.0 INTRODUCTION

This report presents the results of fatigue tests conducted on Nickel-200 alloy specimens to obtain low cycle fatigue performance data for this type of material. The potential application was the replacement of Hastelloy X with Nickel-200 for the hot surface face sheet, in regions of high heat flux. The combined benefits of improved ductility and markedly higher thermal conductivity were believed to offer decidely increased cycle life for the required application.

2.0 TEST SPECIMENS

Solid bar and plate-fin test specimens were prepared for use in the mechanical bending test apparatus that was employed during the low cycle fatigue evaluation for NASA Contract No. NAS1-5002 (Study of Regeneratively Cooled Panels). The solid bar specimens were two inches wide by six in. long, and approximately 0.235 in. thick. The plate-fin specimens used two by six by 0.220 in. thick Hastelloy bars that were recessed on both faces to accept 0.075 in. high rectangular offset fins, which were also made from Hastelloy X. Surface plates of 0.025 in. thick Nickel-200 material were applied to the specimens which were then brazed with Palniro 4 filler alloy. The reduced strength of Nickel-200 necessitated the use of 0.025 in. thick face sheets in comparison with 0.015 in. thick for Hastelloy X, to provide adequate pressure containment strength.

3.0 RESULTS AND DATA REDUCTION

Tests were performed at room temperature and at 1400°F on the solid bars and the plate fin specimens. The 1400°F temperature was representative of nickel face sheet operating conditions when used as a direct replacement for Hastelloy X at the $M_\infty = 8.0$ design point. The test specimens were subjected to fully reversed bending deformations by using formed mandrels of 5, 9, and 16 in. radii to obtain different values of controlled total strain amplitude. The test results for the solid bars are presented in Table I and for the plate-fin specimens on Table 2. Test temperature, specimen thickness, initial load, cyclicly stabilized load, mandrel size and cycles to failure are listed in these tables, following.

Curves were developed using actual room temperature and 1400°F stress-strain data obtained from tensile specimens. Curves were plotted for equivalent plastic strain ranges versus axial total strain range for unaxial loading; two-to-one biaxial loading and equi-biaxial loading. The decreased elastic modulus at elevated temperature corresponded quite closely to the decreased strength, and the curves for plastic strain range versus total strain range were found to be virtually identical at room temperature and at 1400°F. The resulting curves are shown on Figure 1.

The formula for total applied strain range expressed in terms of mandrel radius, R, and specimen thickness, t, is:

$$\epsilon_{tot} = \frac{t}{R + t/2}$$

Using this formula, the total strain ranges applied to the various specimens were computed:

- Solid Bar Specimens

  (a) R = 5 in., h = 0.235 in.

  $$\epsilon_{tot} = \frac{0.235}{5.118} = 0.0460 \text{ in./in.}$$

  $$\Delta\epsilon_{eQ} = 0.0507 \text{ in./in.} \text{ (from Figure 1)}$$

TABLE I

NICKEL-200 SOLID BAR FIXTURE TEST RESULTS

Specimen No.	Test Temp., °F	Specimen Thickness, in.	Initial Load lb.	Stabilized Load lb.	Mandrel Radius, in.	Cycles to Fail	Remarks
1	amb.	0.234	22-50	-	5	67	
2	amb.	0.234	1800	2200	5	72	
3	amb.	0.234	1350	1600	16	1144	
4	1400	0.235	400	-	5	149	Insufficient load - test invalid
5	amb.	0.235	1200	1600	16	1071	
6	1400	0.234	450	600	16	223	
7	1400	0.234	600	Dropped to 225	5	200	Defective test
8	1400	0.236	600	-	16	373	
9	amb.	0.236	1775	2050	9	264	
10	amb.	0.233	1700	600	16	287	
11	1400	0.234	575	600	16	287	
12	1400	0.234	600	600	9	65	
13	1400	0.234	700	700	16	275	
14	1400	0.236	625	625	9	132	
15	1400	0.236	625	625	9	120+	Specimen partially fractured

TABLE 2

NICKEL-200 PLATE-FIN FATIGUE TEST RESULTS

Specimen No.	Test Temp., °F	Specimen Thickness, in.	Initial Load lb.	Stabilized Load, lb.	Mandrel Radius, in.	Cycles to Fail
16 Top	amb.	0.269	1000	1300	9	29
16 Bottom						26
17 Top	amb.	0.268	800	1200	16	132
17 Bottom						130
18 Top	amb.	0.268	800	1200	16	133
18 Bottom						131
19 Top	amb.	0.268	950	1350	9	32
19 Bottom						28
20 Top	1400	0.268	450	600	16	108
20 Bottom						Defective
21 Top	1400	0.269	600	700	9	44
21 Bottom						37
22 Top	1400	0.270	400	550	16	109
22 Bottom						133
23 Top	1400	0.270	550	650	9	39
23 Bottom						31

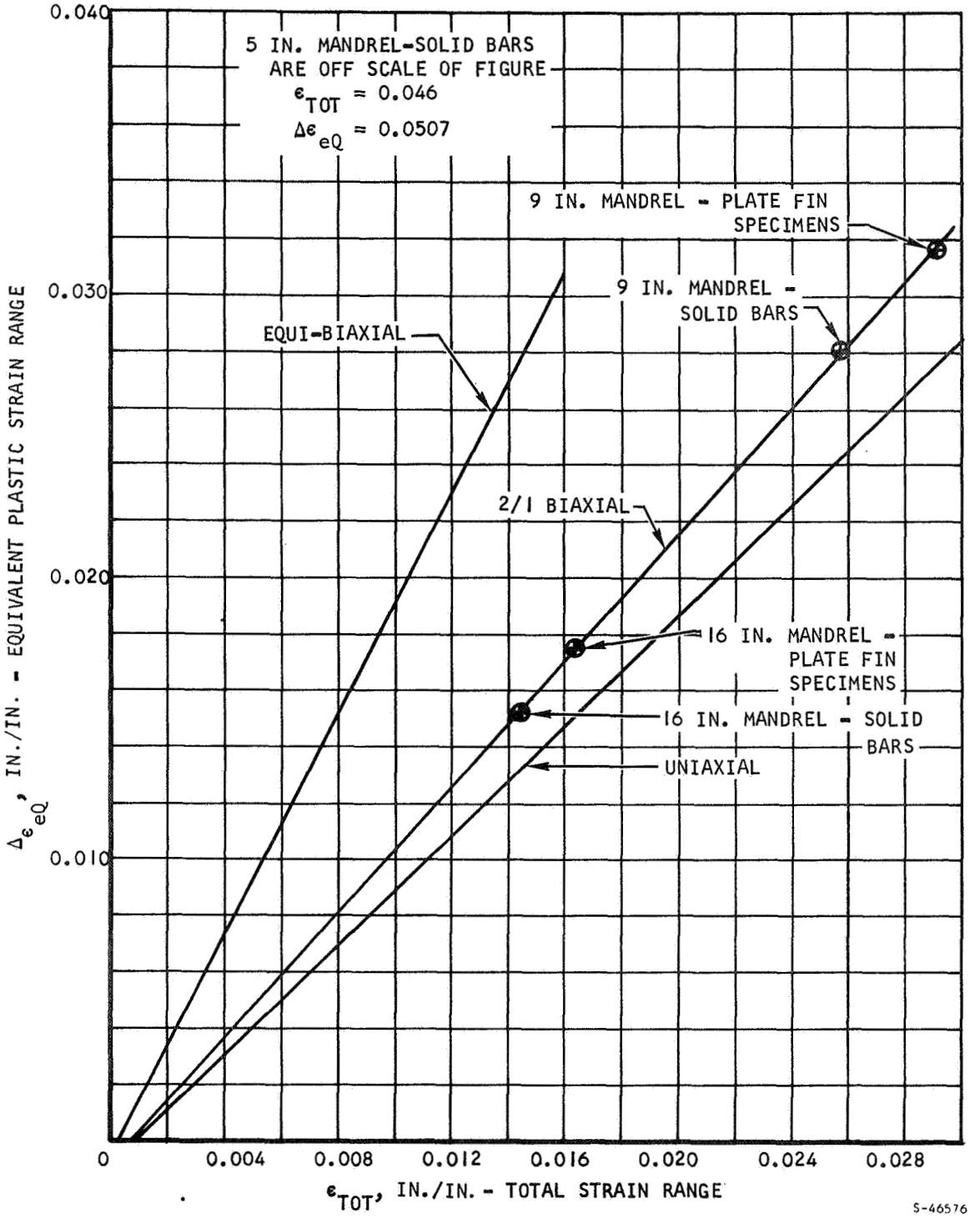

Figure 1. Plastic Strain Range vs ϵ_{TOT} for Nickel-200

(b) R = 9 in.; h = 0.235 in.

$$\epsilon_{tot} = \frac{0.235}{9.118} = 0.0258 \text{ in./in.}$$

$\Delta\epsilon_{eQ}$ = 0.0280 in./in. (from Figure 1)

(c) R = 16 in.; h = 0.235 in.

$$\epsilon_{tot} = \frac{0.235}{16.118} = 0.0145 \text{ in.}$$

$\Delta\epsilon_{eQ}$ = 0.0153 in./in. (from Figure 1)

Plate-Fin Specimens

(a) R = 9 in.; h = 0.270 in.

$$\epsilon_{tot} = \frac{0.270}{9.135} = 0.0292 \text{ in./in.}$$

$\Delta\epsilon_{eQ}$ = 0.0315 in./in. (from Figure)

(b) R = 16 in.; h = 0.270 in.

$$\epsilon_{tot} = \frac{0.270}{16.135} = 0.0165 \text{ in./in.}$$

$\Delta\epsilon_{ea}$ = 0.0175 in./in. (from Figure 1)

These plastic strain ranges were used in conjunction with the test results provided in Tables 1 and 2, to produce the graphical presentation shown in Figure 2. The solid bar test data indicated a reduction in cycles to failure at 1400°F by comparison to the RT results. Nevertheless, the slope of the line for plastic strain range vs cycles is steeper at 1400°F than at RT. Extension of this line in the direction of higher plastic strain range would cause it to intersect the RT line at approximately seven percent plastic strain range (25-30 cycles to fail). This indicates an increase in ductility at 1400°F, which is consistent with tensile data. The steeper slope at 1400°F is attributable to the increased creep contribution to specimen failure at lower strain ranges.

The trends obtained with the plate fin specimens were similar to solid bar data with increased life at 1400°F, a high plastic strain range and a steeper slope in comparison to RT data. The 1400°F and RT lines intersect at approximately two percent strain range (75 cycles to fail). Although not exactly identical, the slopes of the RT lines for the solid bar specimens and the plate fin specimens were in good agreement. The slope of the 1400°F line for the solid bars was definitely steeper than the plate fin line at 1400°F. This is

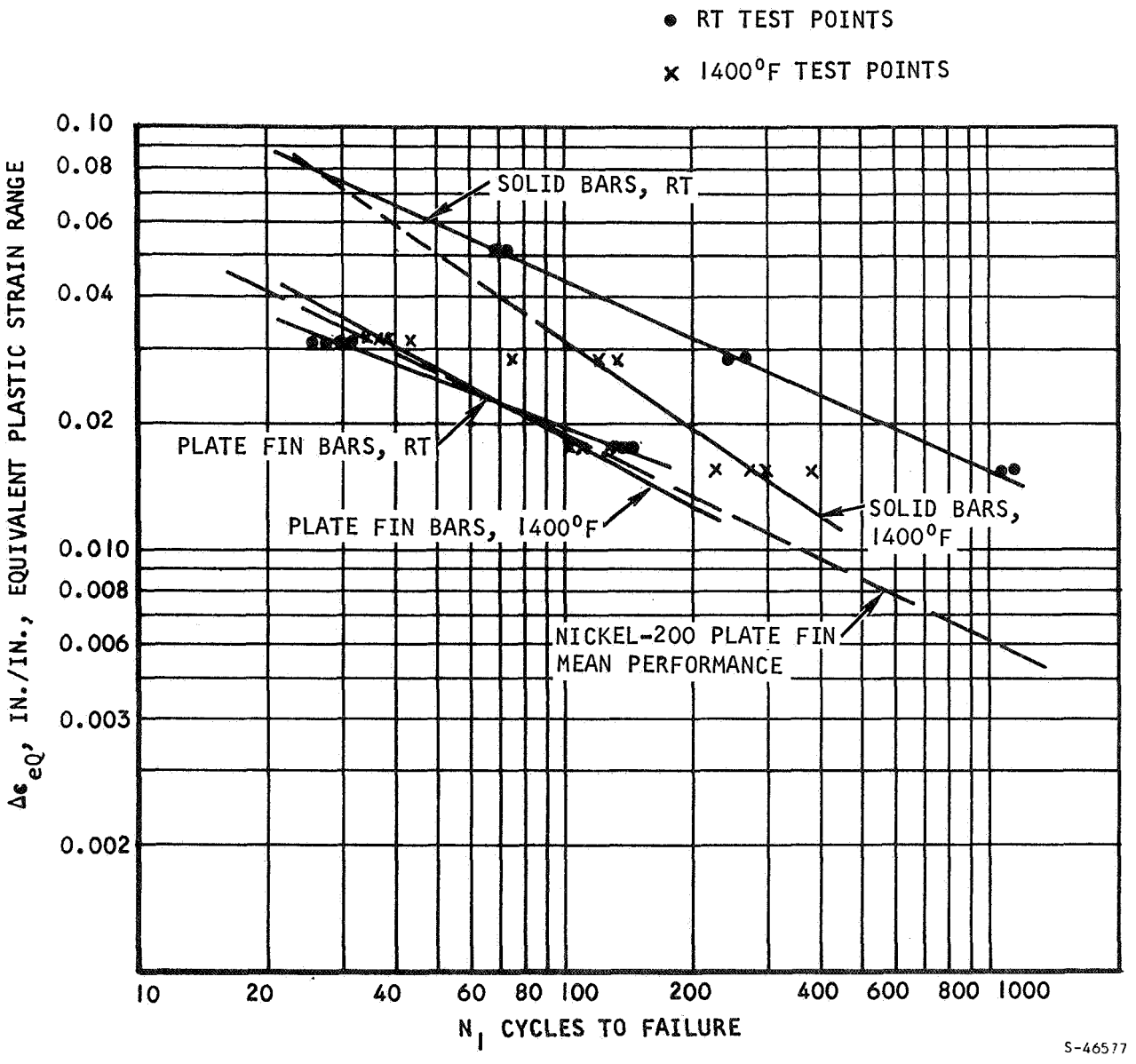

Figure 2. Nickel-200 Fatigue Test Results

at least partially explainable by the difference in test speed with a cyclic rate of two to four full cycles per min. on the solid bars and fifteen to twenty cycles per min. on the plate fin bars. In addition, a substantially higher cycle life with the solid bars produced more accumulated creep strain than with the plate fin bars. Both of these factors lead to increased cumulative creep in the solid bars, and hence a steeper slope in the test lines.

The next and final step in the data reduction was the application of the test results in Figure 2. This was directed toward an estimation of cyclic fatigue engine life as a function of operating temperature differentials between the hot skin and the nickel plate fin hot face sheet. The task was accomplished by taking 1450°F as the reference temperature for a nickel hot outer surface, and by computing the thermal differential growth between the hot surface and the Hastelloy X cold structure for various ΔT values. The elastic deformation of the cold wall during each full cycle was then deducted from the thermal differential growth to obtain the applied strain for the nickel surface. Allowing for the difference in metal thicknesses of the nickel surface wall (0.025 in.) and the Hastelloy X prime structural wall (0.060 in.), and also accounting for the differences in the strength of Nickel-200 at RT and 1450°F, the equi-biaxial elastic strain range applied to the cold wall was computed to be approximately 0.00020 in./in. during each full cycle. The thermal expansion for nickel in heating up from 70° to 1450°F was computed to be $(\alpha\Delta T)_h = (9.0 \times 10^{-6})\ (1450 - 70) = 0.01240$ in./in. The thermal growth of the cold wall was calculated for cold wall temperatures ranging from 1300° down to 500°F (corresponding to ΔT values from 150° to 950°F). The thermal differential growth was calculated as:

$$\Delta\epsilon_{thermal} = \Delta\epsilon_{th} = (\alpha\Delta T)_h - (\alpha\Delta T)_c$$

The applied biaxial strain range to the nickel hot surface was computed by subtracting the cold wall deformation range as follows:

$$\epsilon_{tot} = \Delta\epsilon_{th} - 0.00020$$

The resulting value for ϵ_{tot} was then used to determine $\Delta\epsilon_{eQ}$ from the equi-biaxial curve on Figure 1. Since part of the plastic strain during each duty cycle occurs at RT and part at elevated temperature, a mean performance line was added to Figure 2 for the plate fin bars. This was used to obtain estimated hot surface fatigue life. The calculations are given in Table 3.

These results are plotted on Figure 3. For direct comparison, curves are also presented on this figure showing the predicted cycle life that would be achieved with a Hastelloy X hot surface sheet. The thermal fatigue curve was based on thermal fatigue testing performed earlier in the HRE program and reported in AiResearch Report AP-68-3813. The mechanical fatigue curve was based upon mechanical bending test data obtained during the course of the low cycle fatigue evaluation, under Contract No. NAS1-5002.

TABLE 3

NICKEL-200 FATIGUE LIFE CALCULATIONS

Engine ΔT, °F	Cold Wall Temperature, °F	$(\alpha\Delta T)_c$	$\Delta\epsilon_{th}$	ϵ_{TOT}	$\Delta\epsilon_{\epsilon Q}$	Cycles to Fail, N
150	1300	0.01070	0.00170	0.00150	0.00230	>1000
250	1200	0.00965	0.00275	0.00255	0.00430	>1000
350	1100	0.00870	0.00370	0.00350	0.00620	800
450	1000	0.00775	0.00465	0.00445	0.00810	480
550	900	0.00680	0.00560	0.00540	0.01000	325
650	800	0.00585	0.00655	0.00635	0.01190	235
750	700	0.00495	0.00745	0.00725	0.01360	180
850	600	0.00410	0.00830	0.00810	0.01530	145
950	500	0.00330	0.00910	0.00890	0.01680	130

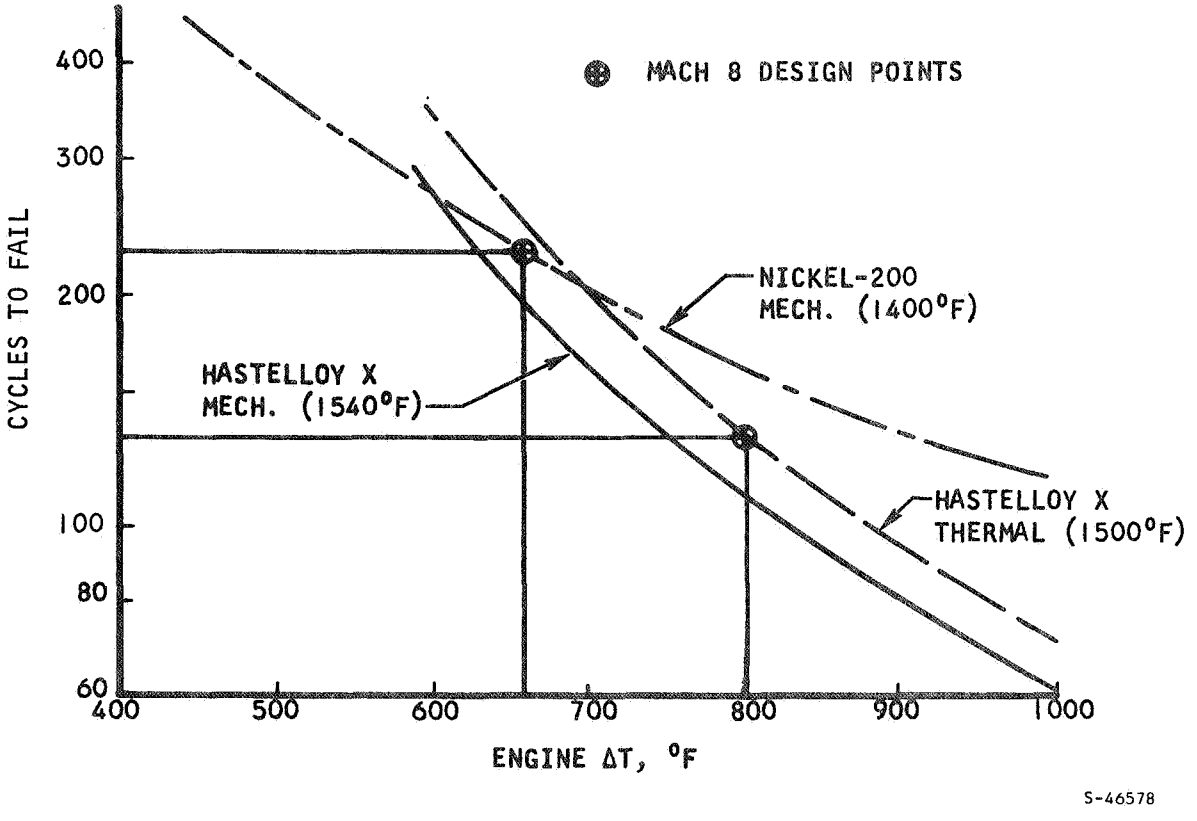

Figure 3. Low Cycle Fatigue
Test Results

4.0 CONCLUSIONS

The appreciably higher strength of Hastelloy X leads to little or no plastic flow with small temperature differentials, and therefore better cycle life than Nickel-200 with small values of engine ΔT. At higher ΔT, the better ductility of Nickel-200 becomes the most important single factor; in spite of the somewhat higher plastic strain range than for Hastelloy X at the same values of ΔT, a greater cycle life is attainable with Nickel-200. The curves in Figure 3 reflect this behavior. Another factor favoring Nickel-200 is the lower ΔT of $662^{\circ}F$ (due to the improved thermal conductivity) compared to $800^{\circ}F$ for 0.015-in. Hastelloy X face sheet at the Mach 8 design point. The actual operating points are indicated on the figure, and an improvement from 136 to 225 cycles is indicated by employing Nickel-200 in place of Hastelloy X, at equal thickness of 0.015 in. For 0.025 in. thick Nickel-200 face sheet, the ΔT increases to $723^{\circ}F$ and the life is reduced to 200 cycles. The relatively low creep-rupture strength of nickel, however, would require further evaluation before the feasibility of employing nickel in this application can be firmly established.